

Polarization and Spectral Shift of Benzophenone in Supercritical Water

T. L. Fonseca*

Instituto de Física, Universidade Federal de Goiás, CP 131, 74001-970 Goiânia, GO, Brazil

H. C. Georg, K. Coutinho, and S. Canuto

Instituto de Física, Universidade de São Paulo, CP 66318, 05315-970 São Paulo, SP, Brazil

Received: November 3, 2008; Revised Manuscript Received: February 18, 2009

Monte Carlo simulation and quantum mechanics calculations based on the INDO/CIS and TD-DFT methods were utilized to study the solvatochromic shift of benzophenone when changing the environment from normal water to supercritical ($P = 340.2$ atm and $T = 673$ K) condition. Solute polarization increases the dipole moment of benzophenone, compared to gas phase, by 88 and 35% in normal and supercritical conditions, giving the in-solvent dipole value of 5.8 and 4.2 D, respectively. The average number of solute–solvent hydrogen bonds was analyzed, and a large decrease of 2.3 in normal water to only 0.8 in the supercritical environment was found. By using these polarized models of benzophenone in the two different conditions of water, we performed MC simulations to generate statistically uncorrelated configurations of the solute surrounded by the solvent molecules and subsequent quantum mechanics calculations on these configurations. When changing from normal to supercritical water environment, INDO/CIS calculations explicitly considering all valence electrons of the 235 solvent water molecules resulted in a solvatochromic shift of 1425 cm^{-1} for the most intense $\pi-\pi^*$ transition of benzophenone, that is, slightly underestimated in comparison with the experimentally inferred result of 1700 cm^{-1} . TD-B3LYP/6-311+G(2d,p) calculations on the same configurations but with benzophenone electrostatically embedded in the 320 water molecules resulted in a solvatochromic shift of 1715 cm^{-1} for this transition, in very good agreement with the experimental result. When using the unpolarized model of the benzophenone, this calculated solvatochromic shift was only 640 cm^{-1} . Additional calculations were also made by using BHandHLYP/6-311+G(2d,p) to analyze the effect of the asymptotic decay of the exchange functional. This study indicates that, contrary to the general expectation, there is a sizable solute polarization even in the low-density regime of supercritical condition and that the inclusion of this polarization is important for a reliable description of the spectral shifts considered here.

1. Introduction

At temperatures and pressures higher than those of the critical point (located at $P_c = 221$ atm and $T_c = 647.3$ K), water becomes a supercritical fluid and exhibits physical and chemical properties that are markedly different from those of normal liquid systems.¹ An important property of supercritical water (SCW) is that its dielectric constant can vary continuously over a wide range of supercritical states, and water becomes an excellent solvent for many organic compounds.¹ This unusual behavior of SCW is a consequence of changes in the electronic and structural properties^{2,3} that, in turn, can be measured spectroscopically by using a probe molecule subjected to the condition that is stable in different thermodynamic conditions. Bennett and Johnston⁴ have used the $n-\pi^*$ transition of acetone and the $\pi-\pi^*$ transition of benzophenone to probe the solute–solvent interactions in SCW. This experiment characterized that, for SCW with $P = 340.2$ atm and $T = 673$ K, the $\pi-\pi^*$ transition of benzophenone suffers a blue shift of 1700 cm^{-1} , compared to the environment of normal water (NW). Under supercritical conditions, only a limited number of theoretical studies on the UV–visible absorption spectrum of probe molecules have been reported.^{5,6} In recent years, methods and algorithms have been developed to study theoretically the

effects of different solvents on the spectral properties of solute molecules⁷ with some emphasis also on solvatochromic shifts.⁸ There is an increasing need for understanding the effect of supercritical environment in the spectroscopic properties of organic molecules. However, the choice has to be made carefully, because there are many organic molecules that are not stable in SCW. In this direction, acetone and benzophenone are simple molecules for which the absorption spectra have been analyzed experimentally,⁴ and theoretical results can be of importance to rationalize solvent effects. We have recently analyzed⁵ the $n-\pi^*$ transition of acetone in SCW in the thermodynamic condition of the existing experimental result. Recently, Lin and Gao⁶ have also investigated the solvatochromic shift of acetone in water but now in a wide range of fluid phases ranging from steam vapor to ambient condition and including supercritical regions. In this present work, we devote our attention to the benzophenone case.

Experimental results for the $n-\pi^*$ and $\pi-\pi^*$ absorption bands of benzophenone in several solvents have been reported by Dilling.⁹ He finds that, from *n*-hexane to water, the strong $\pi-\pi^*$ transition shifts to the red by 1600 cm^{-1} , whereas the $n-\pi^*$ transition in the longer-wavelength region shifts to the blue by 2200 cm^{-1} . Because of the low polarity of *n*-hexane, these shifts are normally taken also as an estimate of the spectral shift from gas phase to aqueous environment. In the absence of gas-phase experiments, one has to resort to estimates. Bennett

* Corresponding author. E-mail: tertius@if.ufg.br, Fax: +55 062.3521-1014.

and Johnston⁵ predict the gas-phase value of the π - π^* absorption band at 41600 cm^{-1} corresponding to a gas \rightarrow NW blue shift of 2600 cm^{-1} . This seems to be a large shift if one considers that it would imply a gas \rightarrow n-hexane shift of ca. 1000 cm^{-1} . From the theoretical point of view, the description of the solvatochromic effects on the n - π^* and π - π^* electronic transitions of benzophenone in aqueous solution is a challenging case because solvation affects these two bands differently, leading to opposite spectral shifts.⁹⁻¹¹ In a previous theoretical work,¹⁰ a discrete solvation model based on the sequential Quantum Mechanics/Molecular Mechanics (S-QM/MM) methodology¹² has been used to calculate the UV-vis spectrum of benzophenone in NW. INDO/CIS calculations on the liquid structures generated by Monte Carlo (MC) simulation with augmented gas-phase atomic charges obtained that the n - π^* transition suffers a blue shift of 1170 cm^{-1} and the π - π^* transition suffers a red shift of 1332 cm^{-1} , in changing from gas to NW. This model thus gives the correct sign for the two absorption shifts but underestimates the results. However, a considerable improvement of the theoretical predictions of UV-vis spectrum of benzophenone in water is achieved by including solute polarization effects.¹¹ For polarized benzophenone, the INDO/CIS model obtained solvatochromic shifts of 2045 cm^{-1} for the n - π^* transition and of -1945 cm^{-1} for the intense π - π^* transition in better agreement with the experimental results. More recently, other theoretical studies have demonstrated the importance of the inclusion of the solute polarization effects in order to obtain a reliable description of the electronic properties of solute molecules in solution.^{11,13,14}

Solute polarization effects are expected to be relatively modest in the supercritical conditions because of the reduced density of the fluid. However, an explicit verification of this assumption is still necessary. In this study, we investigate the solvent effects on the entire UV-vis spectrum of benzophenone in normal and SCW and compare the resulting effects of the solute polarizations in the two environments. Solute polarization has been of great interest and can be included by using different procedures.¹⁴⁻¹⁷ Here, we used an iterative procedure that electrostatically equilibrates the solute in the solvent environment.¹⁵ For each step of the iterative process, we have used an electrostatic embedding described by an average solvent electrostatic configuration (ASEC) to calculate the dipole moment of the solute with just one QM calculation. This single value reproduces the averaged value calculated for a set of statistically uncorrelated configurations that gives a converged result.¹⁶ The procedure we use is similar to that developed by Aguilar and co-workers,¹⁷ except that we use an average configuration instead of an average potential, as described before.¹⁶ Another interesting procedure has been developed by Gao et al.¹⁸ that also uses an average electrostatic potential. After consideration of the solute polarization, we study the electronic transitions. This will be done by using both an all-valence electron approach with INDO/CIS¹⁹ and a time-dependent density-functional theory (TD-DFT)²⁰ where the solvent is treated as an electrostatic embedding. The focus here is to obtain the spectral shift from normal to supercritical thermodynamic condition. In both conditions, we use a polarized solute and analyze the results. The benzophenone spectrum is then calculated in both NW and SCW environments. The INDO/CIS calculations in NW reproduce the results of ref 9. The applicability of the INDO/CIS and TD-DFT approaches for calculating spectral shifts of organic molecules containing the carbonyl (C=O) group in aqueous solution has been successfully reported in the literature.²¹⁻²⁴

2. Computational Details

The MC simulations were performed by using the DICE program²⁵ in the isothermal-isobaric, NPT , ensemble for one benzophenone and 903 water molecules, where the number of molecules N , the pressure P , and the temperature T are fixed. To compare with the experimental SC condition described above,⁵ we have considered $P = 340.2\text{ atm}$ and $T = 673\text{ K}$. Intermolecular interactions were modeled by the standard Lennard-Jones and Coulomb potential with three parameters for each interacting site. For water, the potential used was the extended simple point charge²⁶ (SPC/E) model because it leads to very good agreement for the critical point of water.²⁷ For benzophenone, we have used the OPLS force field,²⁸ and initially, the atomic charges were obtained by using an electrostatic potential fit (CHELPG)²⁹ from a MP2/6-31++G(d,p) gas-phase calculation. All molecules are kept with rigid geometry. The solute geometry used in all MC simulations was optimized in gas phase at the MP2/6-31G level of calculation and was already reported in previous works.^{10,11} In this study, we have not attempted to reoptimize the geometry of benzophenone in the two solvent environments. All QM calculations were performed by using GAUSSIAN 03,³⁰ except the INDO/CIS calculations that were performed with the original ZINDO program.³¹

To account for the solute electronic polarization, we have used the iterative procedure¹⁵ based on the S-QM/MM methodology to determine the in-solution dipole moment of benzophenone in supercritical condition. It is assumed as a reasonable approximation that the reverse, the solvent polarization by the solute, is of less significance. This has been addressed in ref 6 for acetone in different fluid densities and suggests that the effect is mild. We start the iterative procedure (iteration 0) by performing a simulation with the Coulombic term of the solute potential described by its vacuum charge distribution. Here, the atomic charges are obtained by using the electrostatic mapping of CHELPG at the MP2/6-31++G(d,p) level of calculation. After the simulation, we perform a statistical analysis and calculate the correlation interval.¹² Then, we select statistically uncorrelated configurations to generate an electrostatic embedding around the solute, calculate a new charge distribution over the solute atoms, and use this new charge distribution to initiate another step of the iterative process. Therefore, another simulation is performed with these new atomic charges of the solute, a new sampling is made, and another set of QM calculations are performed to obtain new values of the atomic charges of the solute. This procedure is repeated until convergence of the solute dipole moment in solution is achieved. Here, we find the convergence criterion of $|\Delta\mu| \leq 0.1\text{ D}$ sufficient. For each iteration, we have used the electrostatic embedding described by the ASEC, which reproduces the statistical average with just one QM calculation.¹⁶ Here, the ASEC is generated with 100 statistically uncorrelated configurations of one benzophenone surrounded by the nearest 320 water molecules. Initially, we project the configurations to superpose the solute in the same Cartesian coordinates. Then, we treat the solvent molecules as atomic point charges of the SPC/E model ($q(\text{O}) = -0.8476$ and $q(\text{H}) = 0.4238$) divided by 100. In this way, each oxygen and hydrogen atom of a water molecule will be described in the electrostatic embedding as a superposition of 100 Cartesian coordinates, each one with a charge of -0.008476 and 0.004238 , respectively.

In the SC condition, the calculation of n - π^* and π - π^* electronic transitions of benzophenone were performed by using the semiempirical singly excited configuration interaction INDO/

TABLE 1: MP2/6-31++G(d,p) Results for the Atomic Charges (e), Obtained with CHELPG Procedure, in the Carbonyl Group and the Dipole Moment (D) of Benzophenone in Water at Supercritical and Normal Conditions, During the Iteration Procedure of Its Polarization^a

iteration step	NW ^b			SCW		
	$q(O)$	$q(C)$	μ	$q(O)$	$q(C)$	μ
0	-0.4570	0.4021	3.11	-0.4570	0.4021	3.11
1	-0.5712	0.4701	4.65	-0.4971	0.4183	3.75
2	-0.6340	0.5112	5.55	0.5151	0.4369	4.00
3	-0.6568	0.5186	5.71	-0.5276	0.4446	4.19
4	0.6636	0.5247	5.84	-0.5216	0.4339	4.19

^aThe calculated values were obtained as average over 100 uncorrelated configurations. ^bReference 11.

CIS¹⁹ method with the spectroscopic parametrization. This will allow the use of a large solvation shell with 235 explicit water molecules. This corresponds to a 2148 valence-electron problem, where the wave function delocalizes over the solvent region and includes part of the dispersion contribution.^{12c} INDO/CIS calculations for the $n-\pi^*$ and $\pi-\pi^*$ transitions in NW have been reported in ref 11. In addition, we have also calculated these electronic transitions in the two different thermodynamic conditions by using the TD-DFT method. TD-DFT transition energies were calculated by using the B3LYP hybrid functional³² with the 6-311+G(2d,p) basis set and a large solvation shell of 320 water molecules treated as simple point charges describing an electrostatic embedding. Absorption spectra in good agreement with experiments have been obtained for a number of solvated organic molecules by using the TD-B3LYP/6-311+G(2d,p) model.³³ Because B3LYP has an incorrect asymptotic behavior for the exchange-correlation potential,³⁴ it has been questioned in a number of recent applications.^{35,36} In this direction, there has been an increasing tendency to use the new Coulomb-attenuating (CAM-B3LYP) variant.³⁷ On the other hand, because the Hartree-Fock (HF) model has the correct asymptotic decay, another tendency has been to increase the participation of the HF exchange part. One of these alternatives is provided by the BHandHLYP that combines HF and Becke88 functionals³⁸ for the exchange part. As we will see below, the calculated excitation energies obtained with BHandHLYP are improved compared to the simple B3LYP, but this model gives essentially the same picture for the solvatochromic shifts. These will be discussed in Sections 3.3 and 3.4.

3. Results and Discussion

3.1. Solute Polarization. Table 1 gives the MP2/6-31++G(d,p) results for the average dipole moment and the atomic charges of the carbonyl group of benzophenone in the supercritical condition obtained by using the iterative procedure described in the previous section. The gas-phase value is obtained here as 3.11 D, in good agreement with the experimental value³⁹ of 2.98 D. The evolution of the dipole moment along the iterative process is illustrated in Figure 1. For comparison, the corresponding results obtained in normal condition have also been included. The faster convergence presented by the dipole moment in SCW (Figure 1) is attributed to the lower density of water in this case. The converged result for the dipole moment of the polarized benzophenone is 4.19 ± 0.10 D in SCW and 5.84 ± 0.10 D in NW. The increase of 35% in the dipole moment of benzophenone in SCW, compared

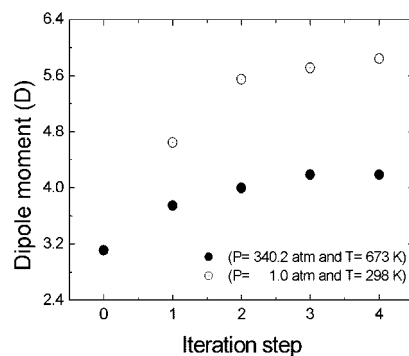


Figure 1. Evolution of the MP2/6-311++G(d,p) results for the dipole moment of benzophenone in water in the supercritical and normal conditions, with respect to the number of iterations for obtaining the solute polarization.

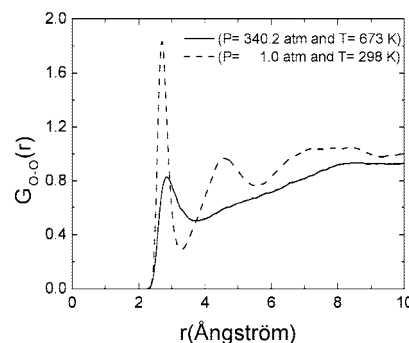


Figure 2. Radial distribution functions between the oxygen atom of benzophenone and the oxygen atom of water in the supercritical and normal conditions. Results obtained after including solute polarization.

to the gas-phase result of 3.11 D, shows that the polarization effects are small compared to the 88% increase in NW, but they are still sizable. Because the SC regime involves a large set of thermodynamic conditions, we characterize the state that we are considering by its density. In the SC condition considered here, the calculated density is $\rho = 0.46 \pm 0.03$ g/cm³, corresponding to the so-called near-critical regime.⁴ Thus, although the density is less than half the density of NW (calculated here as 1.02 ± 0.01 g/cm³), the solute polarization is important and should have an important influence on the spectroscopic properties. For comparison, the corresponding increase for the dipole moment of the acetone predicted by the B3LYP/6-311++G(2d,2p) model is 27% in SCW and 63% in NW.⁴⁰ Before we discuss the spectral shifts, it is interesting to analyze the structure of water molecules around the benzophenone molecule. The MC simulations will now use the converged values for the solute charge, thus including the polarization effects. This corresponds to a dipole moment of benzophenone of 4.2 D in SCW and 5.8 D in NW.

3.2. Solute-Solvent Structure. An important aspect of SCW is the decrease in the number of hydrogen bonds (HB). Here, we briefly analyze the solute-solvent HB and the structure of water molecules around benzophenone. Figure 2 shows the radial distribution functions between the oxygen of the polarized benzophenone and the oxygen of water, $G_{O-O}(r)$, in the supercritical condition and in the normal condition. At SC condition, there is a clear peak centered at 2.85 Å that corresponds to the solute-solvent HB shell. However, there are significant structural changes of the first coordination shell of the benzophenone in changing from NW to SCW, indicating that the average number of water molecules that are hydrogen-

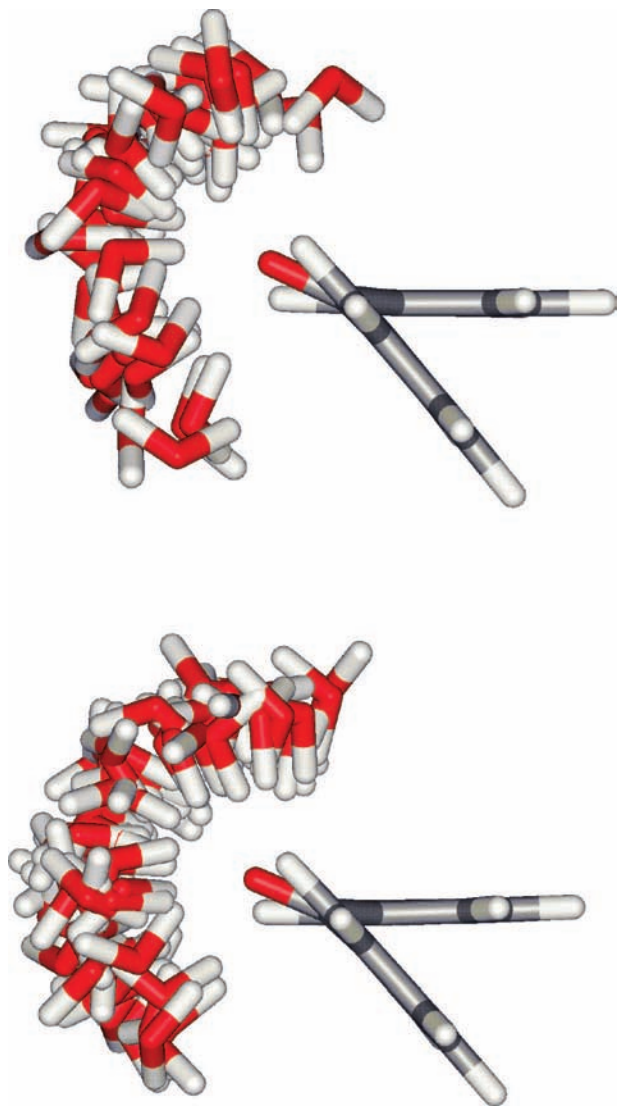


Figure 3. Superposition of the configurations showing HB of unpolarized (top) and polarized (bottom) benzophenone in SCW.

bonded to benzophenone is sensitively reduced in the SC condition. To quantify the number of HB involved, we use here a geometric and energetic criteria defined at ambient conditions to select the hydrogen-bonded molecules.^{21,23,41} Thus, the HB are defined when the separation $R_{O\cdots O} \leq 3.5 \text{ \AA}$ (first minimum of the radial distribution function) and the angle $\theta_{O\cdots O-H} \leq 40^\circ$ and when the solute–solvent interaction energy is at least -2.0 kcal/mol (inferred from the pairwise solute–solvent energy distribution). First, we analyze the effect of the solute polarization in the number of solute–solvent HB. By using 100 uncorrelated MC configurations, our statistical analysis of HB for polarized benzophenone in SCW shows that 32% of the configurations make no HB, 54% form one HB, and 14% make two HB. In the unpolarized case, these numbers are, respectively, 54, 40, and 6%. There are no configurations with three or more HB. In both cases, the statistics thus implies that the most probable number of HB is simply one, but the average number of HB is 0.8 for the polarized and 0.5 for the unpolarized situations. Figure 3 shows the configuration space spanned by the neighboring water molecules that are involved in benzophenone–water HB. When comparing with the unpolarized results, we note that the number of solute–solvent HB in the polarized solute increases, but these numbers are, as expected, smaller than that for NW in the polarized case that gives a total of 2.3

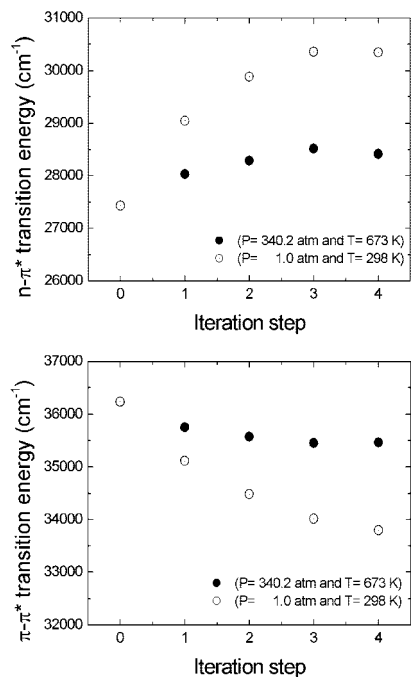


Figure 4. Convergence of the TD-B3LYP/6-311+G(2d,p) results for the $n-\pi^*$ (top) and the most intense $\pi-\pi^*$ (bottom) electronic transitions of benzophenone in water at supercritical and normal conditions, during the iterative procedure for including solute polarization.

HB. For the polarized benzophenone, the change of the thermodynamic conditions from NW to SCW thus leads to a marked reduction of 64% (from 2.3 to 0.8) in the number of HB.

3.3. Polarization Effects on the Transition Energies. We now analyze the absorption spectrum of benzophenone in SCW. In Figure 4 are presented the statistically converged TD-B3LYP/6-311+G(2d,p) results for the $n-\pi^*$ and $\pi-\pi^*$ transitions of benzophenone obtained in SCW and in NW as a function of the number of iterations used in the polarization procedure. These spectroscopic properties were obtained with the benzophenone embedded in the electrostatic field of the outer solvation shell composed of 320 water molecules treated as simple point charges of the SPC/E model. One can see that the electrostatic interactions with the solvent molecules during the iterative process affect the $\pi-\pi^*$ and $n-\pi^*$ transitions in SC condition, but their impact is larger in the NW condition. In comparison with the result of gas phase, the $\pi-\pi^*$ red shifts for the unpolarized and polarized benzophenone are, respectively, -480 and -770 cm^{-1} for SCW and of -1120 and -2485 cm^{-1} for NW. The TD-B3LYP results thus reveal that the $n-\pi^*$ transition is slightly more affected by the solute polarization than the $\pi-\pi^*$. For the $n-\pi^*$ transition, the calculated blue shifts are 600 cm^{-1} in the unpolarized case and 985 cm^{-1} in the polarized case for the SCW environment. For NW, these values are, respectively, 1620 and 2955 cm^{-1} . The solute polarization improves the agreement with experiments and leads to an increase of ca. 60% in the SCW for both transitions. The TD-B3LYP absorption energies for the most intense and characteristic $\pi-\pi^*$ transition of the polarized benzophenone is 35470 cm^{-1} for SCW and of 33755 cm^{-1} for NW, giving a theoretical NW \rightarrow SCW spectral shift value of 1715 cm^{-1} . This shows a decrease in energy transition with increasing water density, in qualitative agreement with the experimental results around 40530 cm^{-1} for SCW⁴ and 38830 cm^{-1} for NW.⁹ As we can see, the calculated transition energies obtained by using

TABLE 2: Solvent Shifts of the Absorption Transitions (cm^{-1}) of Polarized Benzophenone Calculated with INDO/CIS^a

transitions	gas phase	NW		SCW		NW \rightarrow SCW shift
		shift	Osc. str.	shift	osc. str.	
$n-\pi^*$	25,390	2045	0.003	590	0.002	-1455
$\pi-\pi^*$	36,160	-245	0.021	-140	0.011	105
$\pi-\pi^*$	36,320	-570	0.027	-45	0.016	525
$\pi-\pi^*$	39,800	-1945	0.257	-520	0.250	1425
$\pi-\pi^*$	40,660	-1360	0.064	-260	0.057	1100

^a Average results obtained by using 100 configurations of one benzophenone surrounded by explicit 235 water molecules.

TD-B3LYP are lower than the experimental results. At this stage, we comment on some results obtained by using the same basis set in the CAM-B3LYP (by using the Dalton program)⁴² and BHandHLYP functional (already implemented in the Gaussian 03 program). In this case, all excitation energies increase compared to B3LYP. For instance, in the gas phase, the most intense and characteristic $\pi-\pi^*$ transition increases by as much as $\sim 4000 \text{ cm}^{-1}$, thus considerably improving the agreement between theory and experiment. In fact, the results obtained in the gas phase by using TD-CAM-B3LYP and TD-BHandHLYP are similar for the $\pi-\pi^*$ transition. The strong $\pi-\pi^*$ transition is calculated at 40140 cm^{-1} by using CAM-B3LYP and 40710 cm^{-1} by using BHandHLYP. In the calculation of the solvatochromic shifts, we use the TD-BHandHLYP/6-311+G(2d,p) model in addition to the TD-B3LYP/6-311+G(2d,p).

The experimental NW \rightarrow SCW spectral shift value of 1700 cm^{-1} is very well reproduced by the present theoretical results after including the solute polarization. Theoretical studies of the polarization effects in supercritical environment and how these affect the spectroscopic properties of a probe molecule are still very scarce. These results are indicative of their importance. But the relative importance of the polarization effects has been noted in the structure of pure water in supercritical conditions.⁴³ Although the TD-B3LYP transition energies are smaller than the experimental values, the spectral shift of interest here is calculated in very good agreement with experiment. This is discussed in more detail in the next section.

3.4. Spectral Shifts. Because of the uncertainty in the transition energy values for the gas phase and for a better comparison of the polarization effects, we analyze the spectral shifts in the supercritical environment by taking NW as the reference, that is, NW \rightarrow SCW spectral shifts. The calculated INDO/CIS, TD-B3LYP/6-311+G(2d,p), and TD-BHandHLYP/6-311+G(2d,p) solvatochromic shifts for the $n-\pi^*$ and $\pi-\pi^*$ transitions of benzophenone in going from normal to SCW are displayed in Tables 2 and 3, respectively. From the statistically uncorrelated configurations obtained by using the unpolarized model for the solute, the TD-B3LYP method gives NW \rightarrow SCW shifts in the $n-\pi^*$ and $\pi-\pi^*$ (more intense) transitions of -1020 and 640 cm^{-1} , respectively. The corresponding shifts for the polarized benzophenone are of -1970 and 1715 cm^{-1} (Table 3). For these transitions, the TD-BHandHLYP model gives NW \rightarrow SCW shifts of -2305 and 2085 cm^{-1} , whereas the INDO/CIS model gives -1455 and 1425 cm^{-1} for the polarized solute. We also note for the TD-BHandHLYP calculations an increase of the intensity of a lower component of the $\pi-\pi^*$ electronic transitions. By taking an intensity weight into consideration, the calculated spectral shift would decrease, improving agreement with experiment. The unpolarized results

TABLE 3: Solvent Shifts of the Absorption Transitions (cm^{-1}) of Polarized Benzophenone Calculated with (Top Entry) TD-B3LYP/6-311+G(2d,p) and (Bottom Entry) BHandHLYP/6-311+G(2d,p)^a

transitions	gas phase	NW		SCW		NW \rightarrow SCW shift
		shift	osc. str.	shift	osc. str.	
	27430	2955	0.0001	985	0.0001	-1970
$n-\pi^*$	31250	3375	0.0007	1070	0.0013	-2305
	34775	-2665	0.016	-870	0.013	1795
$\pi-\pi^*$	39700	-2320	0.028	-685	0.022	1635
	35425	-2780	0.023	-850	0.036	1930
$\pi-\pi^*$	40170	-2075	0.147	-645	0.154	1430
	36240	-2485	0.360	-770	0.302	1715
$\pi-\pi^*$	40710	-2880	0.305	-795	0.258	2085
	37815	-1215	0.054	-360	0.050	855
$\pi-\pi^*$	41950	-1120	0.069	-325	0.064	795

^a These results are obtained by using the solute electrostatically embedded in 320 water molecules treated as SPC/E point charges.

predicted for these transitions are too small, indicating that the solute polarization effects are thus very important for the reliable prediction of spectral shifts in different thermodynamic conditions. The results based on the TD-DFT calculation for the solvatochromic shift of the most intense $\pi-\pi^*$ transition in the polarized situation is 1715 cm^{-1} (B3LYP) and 2085 cm^{-1} (BHandHLYP), in very good agreement with the available experimental result of 1700 cm^{-1} . The INDO/CIS model gives the corresponding value of 1425 cm^{-1} , which is a slightly underestimated result, but still in good agreement with experiment. The location of the $\pi-\pi^*$ transition of benzophenone in the gas phase is unknown. The INDO/CIS model obtains a value of -1945 cm^{-1} for the gas \rightarrow NW shift, which is close to the experimental result of -1600 for n-hexane \rightarrow NW. The corresponding TD-B3LYP value is -2440 cm^{-1} , which is now closer to the prediction of -2600 cm^{-1} of Bennett and Johnston.⁴ In the case of the $n-\pi^*$ transition, the findings also show a dependence with the inclusion of solute polarization effects; but unfortunately, this has not been reported in the SCW experimental study,⁴ and we could not find the corresponding experimental result for comparison.

The $\pi-\pi^*$ absorption transition of benzophenone in water is in fact a broad and intense band in the region of 260 nm and exhibits a shoulder⁹ at a larger wavelength. An interesting feature of the spectra is that this shoulder is demonstrated to be enclosed by the intense band when going from n-hexane to methanol. This suggests that the transitions responsible for the shoulder suffer a smaller red shift, with increasing solvent polarity, compared to the intense band. Up to this point, we have been comparing the theoretical results with the intensity maximum. As Tables 2 and 3 show, there are four calculated $\pi-\pi^*$ transitions in this region. The two last transitions are the most intense and correspond to the intense band, whereas the first two are mild and correspond to the shoulder. The positions of the four transitions calculated with INDO/CIS also agree very well with the experimental data, whereas the TD-DFT $\pi-\pi^*$ transitions are somewhat underestimated. From Tables 2 and 3, we note that the shifts of the transitions corresponding to the shoulder are considerably smaller than the intense transitions when calculated with INDO/CIS, for both NW and SCW. On the other hand, the shifts obtained with TD-DFT are almost all of comparable size, except for the last transition, for both thermodynamic conditions.

Now, a complete comparison with experiment should consider the contribution of these four transitions to the spectral band.

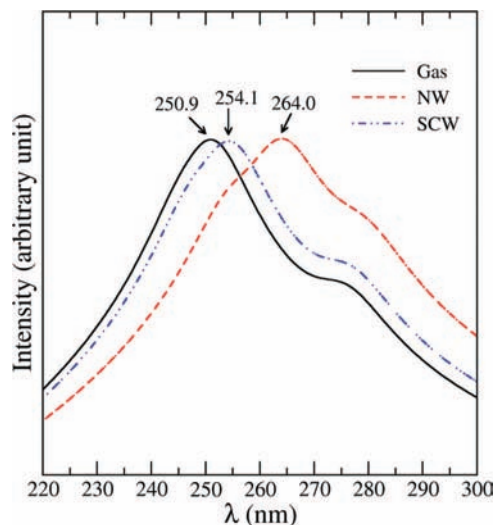


Figure 5. Calculated π - π^* absorption band in the gas phase in NW and SCW. The NW-SCW spectral shift is 9.9 nm, corresponding to 1470 cm^{-1} .

This can be made by convoluting the theoretical results by using the transition energies and the corresponding intensities (obtained from the calculated oscillator strengths). To simulate the spectrum, we have used individual line widths of 1000 cm^{-1} for each calculated transition. The result is shown in Figure 5 by using the INDO/CIS results presented in Table 2. The qualitative agreement is excellent if one compares the solvent effects on the experimental band shifts.⁹ The shift of the band maximum is essentially the same as the one obtained in Table 2 ($1470\text{ vs }1425\text{ cm}^{-1}$), but the solvent effect in the shoulder adds a qualitative agreement that is not found in the DFT calculations, where the calculated shoulder shift is much more pronounced.

4. Conclusion

The electronic transitions of benzophenone in supercritical and normal conditions have been determined theoretically by using Metropolis *NPT* Monte Carlo simulation and quantum mechanics calculations based on INDO/CIS and TD-B3LYP/6-311+G(2d,p) methods. To give some attention to the wrong asymptotic decay of the B3LYP exchange-correlation potential, the calculations were also done by using the half-and-half BHandHLYP functional. The supercritical parameters adopted are those of the experimental study ($P = 340.2\text{ atm}$ and $T = 673\text{ K}$). The solute polarization by the solvent in the supercritical environment has been included by using an iterative procedure. On the basis of MP2/6-311+G(d,p) calculations, an increase of 35% is obtained for the dipole moment of benzophenone in SCW compared to the gas-phase situation. This corresponds to a dipole moment of 4.2 D in the supercritical state that is calculated to have a density of 0.46 g/cm^3 . Thus, even in the supercritical condition, the solute polarization effects are significant, and quantitative estimates of the spectral shifts on the n - π^* and π - π^* electronic transitions require the use of a polarized solute model. For the intense π - π^* transition of polarized benzophenone, the TD-B3LYP/6-311+G(2d,p) model gives an underestimated excitation energy but predicts a solvatochromic shift of the band maximum of 1715 cm^{-1} , changing from normal to supercritical condition, in excellent agreement with the inferred experimental result of 1700 cm^{-1} . In this case, the INDO/CIS model gives a good but slightly underestimated result of 1425 cm^{-1} , whereas the TD-BHandH-

LYP gives instead a good but slightly overestimated result of 2085 cm^{-1} . However, the absolute values of the transitions and the qualitative behavior of the spectral shift of the π - π^* absorption bands is well reproduced in the TD-BHandHLYP calculations. This study suggests that solute polarization could be more important than expected for a reliable description of the solvent effects, even in the low-density regime of the supercritical states of water.

Acknowledgment. This work has been partially supported by CNPq, CAPES/PROCAD, and FAPESP (Brazil). T.L.F. thanks FAPESP and CAPES/PROCAD for providing financial support to visit the Institute of Physics, USP, in different occasions. We thank Prof. Benedito J. C. Cabral for discussions.

References and Notes

- (1) (a) Toker, S. C. *Chem. Rev.* **1999**, *99*, 391. (b) Savage, P. E. *Chem. Rev.* **1999**, *99*, 603.
- (2) (a) Mountain, R. D. *J. Chem. Phys.* **1989**, *90*, 1866. (b) Tromp, R. H.; Postorino, P.; Neilson, G. W.; Ricci, M. A.; Soper, A. K. *J. Chem. Phys.* **1994**, *101*, 6210. (c) Gorbaty, Y. E.; Kalinichev, A. G. *J. Phys. Chem.* **1995**, *99*, 5336. (d) Mizan, T. I.; Savage, P. E.; Ziff, R. M. *J. Phys. Chem.* **1996**, *100*, 403. (e) Bellissent-Funel, M.-C.; Tassaing, T.; Zhao, H.; Beysens, D.; Guillot, B.; Guissani, Y. *J. Chem. Phys.* **1997**, *107*, 2942. (f) Tassaing, T.; Bellissent-Funel, M. C.; Guillot, B.; Guissani, Y. *Europhys. Lett.* **1998**, *42*, 265. (g) Matubayasi, N.; Wakai, C.; Nakahara, M. *Phys. Rev. Lett.* **1997**, *78*, 2573. (h) Soper, A. K.; Bruni, F.; Ricci, M. A. *J. Chem. Phys.* **1997**, *106*, 247. (i) Hoffmann, M. M.; Conradi, M. S. *J. Am. Chem. Soc.* **1997**, *119*, 3811.
- (3) Chialvo, A. A.; Cummings, P. T.; Simonson, J. M.; Mesmer, R. E.; Cochran, H. D. *Ind. Eng. Chem. Res.* **1998**, *37*, 3021.
- (4) Bennett, G. E.; Johnston, K. P. *J. Phys. Chem.* **1994**, *98*, 441.
- (5) Fonseca, T. L.; Coutinho, K.; Canuto, S. *J. Chem. Phys.* **2007**, *126*, 034508.
- (6) Lin, Y. L.; Gao, J. *J. Chem. Theory Comput.* **2007**, *3*, 1484.
- (7) (a) Mennucci, B.; Cammi, R., Eds. *Continuum Solvation Models in Chemical Physics*; Wiley, 2007. (b) Canuto, S., Ed. *Solvation Effects on Molecules and Biomolecules. Computational Methods and Applications*; Springer, 2008.
- (8) (a) Blair, J. T.; Krogh-Jespersen, K.; Levy, R. M. *J. Am. Chem. Soc.* **1989**, *111*, 6948. (b) Gao, J. *J. Am. Chem. Soc.* **1994**, *116*, 9324. (c) Gao, J. In *Reviews of Computational Chemistry*; Lipkowitz, K. B., Boyd, D. B., Eds.; VCH, New York, 1996; Vol. 7, p 119. (d) Kongsted, J.; Osted, A.; Mikkelsen, K.; Chistiansen, O. *J. Chem. Phys.* **2003**, *119*, 10519. (e) Mennucci, B.; Martinez, J. M.; Tomasi, J. *J. Phys. Chem. A* **2001**, *105*, 7287. (f) Miertus, S.; Scrocco, E.; Tomasi, J. *J. Chem. Phys.* **1981**, *55*, 117. (g) Mikkelsen, K. V.; Ågren, H.; Jensen, H. J. A.; Helgaker, T. *J. Chem. Phys.* **1988**, *89*, 3086. (h) Orozco, M.; Luque, F. J. *J. Chem. Rev.* **2000**, *100*, 4187. (i) Öhrn, A.; Karlström, G. *Mol. Phys.* **2006**, *104*, 3087. (j) Sánchez, M. L.; Aguilar, M. A.; Olivares Del Valle, F. J. *J. Comput. Chem.* **1997**, *18*, 313. (k) Ten-no, S.; Hirata, F.; Kato, S. *J. Chem. Phys.* **1994**, *100*, 7443. (l) Zeng, J.; Craw, J. S.; Hush, N. S.; Reimers, J. R. *J. Phys. Chem.* **1993**, *98*, 11075.
- (9) Dilling, W. L. *J. Org. Chem.* **1966**, *31*, 1045.
- (10) Urahata, S.; Canuto, S. *Int. J. Quantum Chem.* **2000**, *80*, 1062.
- (11) Georg, H. C.; Coutinho, K.; Canuto, S. *J. Chem. Phys.* **2007**, *126*, 034507.
- (12) (a) Coutinho, K.; Canuto, S. *Adv. Quantum Chem.* **1997**, *28*, 89. (b) Coutinho, K.; Canuto, S. *J. Chem. Phys.* **2000**, *113*, 9132. (c) Canuto, S.; Coutinho, K.; Zerner, M. C. *J. Chem. Phys.* **2000**, *112*, 7293.
- (13) Ludwig, V.; Coutinho, K.; Canuto, S. *Phys. Chem. Chem. Phys.* **2007**, *9*, 4907.
- (14) (a) Jorgensen, W. L. ed. *J. Chem. Theory Comput.* special issue 6, 2007, 3, pp 1877-2145; (b) Cramer, C. J.; Truhlar, D. G. *Science* **1992**, *256*, 213. (c) Kongsted, J.; Osted, A.; Mikkelsen, K. V.; Christiansen, O. *Chem. Phys. Lett.* **2002**, *364*, 379. (d) Wallqvist, A.; Ahlström, P.; Karlström, G. *J. Phys. Chem.* **1990**, *94*, 1649. (e) McDonald, N. A.; Carlson, H. A.; Jorgensen, W. L. *J. Phys. Org. Chem.* **1997**, *10*, 563. (f) Warshell, A.; Kato, M.; Pislakov, A. V. *J. Chem. Theory Comput.* **2007**, *3*, 2034. (g) Martin, M. E.; Sánchez, M. L.; Oliveira del Valle, F. J.; Aguilar, M. A. *J. Chem. Phys.* **2000**, *113*, 6308.
- (15) Georg, H. C.; Coutinho, K.; Canuto, S. *Chem. Phys. Lett.* **2006**, *429*, 119.
- (16) Coutinho, K.; Georg, H. C.; Fonseca, T. L.; Ludwig, V.; Canuto, S. *Chem. Phys. Lett.* **2007**, *437*, 148.
- (17) Sánchez, M. L.; Aguilar, M. A.; Olivares Del Valle, F. J. *J. Comput. Chem.* **1997**, *18*, 313.
- (18) Gao, J.; Luque, F. J.; Orozco, M. *J. Chem. Phys.* **1993**, *98*, 2975.

- (19) Ridley, J.; Zerner, M. C. *Theor. Chim. Acta* **1973**, *32*, 111.
- (20) Runge, E.; Gross, E. K. U. *Phys. Rev. Lett.* **1984**, *52*, 997.
- (21) Coutinho, K.; Canuto, S. *J. Mol. Struct. (Theochem)* **2003**, *632*, 235.
- (22) Röhrig, U. F.; Frank, I.; Hutter, J.; Laio, A.; Vandevondele, J.; Rothlisberger, U. *Chem. Phys. Chem.* **2003**, *4*, 1177.
- (23) Georg, H. C.; Coutinho, K.; Canuto, S. *J. Chem. Phys.* **2005**, *123*, 124307.
- (24) Sulpizi, M.; Röhrig, U. F.; Hutter, J.; Rothlisberger, U. *Int. J. Quantum Chem.* **2005**, *101*, 671.
- (25) Coutinho, K.; Canuto, S. *DICE: A Monte Carlo program for molecular liquid simulation*, version 2.8; University of São Paulo: São Paulo, 2003.
- (26) Berendsen, H. J. C.; Grigera, J. R.; Straatsma, T. P. *J. Phys. Chem.* **1987**, *91*, 6269.
- (27) (a) Guissani, Y.; Guillot, B. *J. Chem. Phys.* **1993**, *98*, 8221. (b) Guillot, B.; Guissani, Y. *J. Chem. Phys.* **1993**, *99*, 8075.
- (28) Jorgensen, W. L.; Maxwell, D. S.; Tirado-Rives, J. *J. Am. Chem. Soc.* **1996**, *118*, 11225.
- (29) Breneman, C. M.; Wiberg, K. B. *J. Comput. Chem.* **1990**, *11*, 361.
- (30) Frisch, M. J.; Trucks, G. W.; Schlegel, H. B.; Scuseria, G. E.; Robb, M. A.; Cheeseman, J. R.; Montgomery, Jr., J. A.; Vreven, T.; Kudin, K. N.; Burant, J. C.; Millam, J. M.; Iyengar, S. S.; Tomasi, J.; Barone, V.; Mennucci, B.; Cossi, M.; Scalmani, G.; Rega, N.; Petersson, G. A.; Nakatsuji, H.; Hada, M.; Ehara, M.; Toyota, K.; Fukuda, R.; Hasegawa, J.; Ishida, M.; Nakajima, T.; Honda, Y.; Kitao, O.; Nakai, H.; Klene, M.; Li, X.; Knox, J. E.; Hratchian, H. P.; Cross, J. B.; Bakken, V.; Adamo, C.; Jaramillo, J.; Gomperts, R.; Stratmann, R. E.; Yazyev, O.; Austin, A. J.; Cammi, R.; Pomelli, C.; Ochterski, J. W.; Ayala, P. Y.; Morokuma, K.; Voth, G. A.; Salvador, P.; Dannenberg, J. J.; Zakrzewski, V. G.; Dapprich, S.; Daniels, A. D.; Strain, M. C.; Farkas, O.; Malick, D. K.; Rabuck, A. D.; Raghavachari, K.; Foresman, J. B.; Ortiz, J. V.; Cui, Q.; Baboul, A. G.; Clifford, S.; Cioslowski, J.; Stefanov, B. B.; Liu, G.; Liashenko, A.; Piskorz, P.; Komaromi, I.; Martin, R. L.; Fox, D. J.; Keith, T.; Al-Laham, M. A.; Peng, C. Y.; Nanayakkara, A.; Challacombe, M.; Gill, P. M. W.; Johnson, B.; Chen, W.; Wong, M. W.; Gonzalez, C.; Pople, J. A. *Gaussian 03, Revision D.01*; Gaussian Inc.: Wallingford CT, 2004.
- (31) Zerner M. C. *ZINDO, A semi-empirical program package*; University of Florida: Gainesville, FL; 32611.
- (32) (a) Lee, C.; Yang, W.; Parr, R. G. *Phys. Rev. B* **1988**, *37*, 785. (b) Becke, A. D. *J. Chem. Phys.* **1993**, *98*, 5648.
- (33) (a) Jacquemin, D.; Preat, J.; Wathélet, V.; Perpète, E. A. *J. Mol. Struct. (Theochem)* **2005**, *731*, 67. (b) Jacquemin, D.; Perpète, E. A. *Chem. Phys. Lett.* **2006**, *429*, 147. (c) Fonseca, T. L.; de Oliveira, H. C. B.; Castro, M. A. *Chem. Phys. Lett.* **2008**, *457*, 119.
- (34) (a) Tozer, D. J.; Handy, N. C. *J. Chem. Phys.* **1998**, *108*, 2545. (b) Tozer, D. J.; Handy, N. C. *Mol. Phys.* **2003**, *101*, 2669. (c) Rohrdanz, M. A.; Martins, K. M.; Herbert, J. M. *J. Chem. Phys.* **2009**, *130*, 054112.
- (35) (a) Bauernschmitt, R.; Ahlrichs, R. *Chem. Phys. Lett.* **1996**, *256*, 454. (b) Tozer, D. J.; Handy, N. C. *J. Chem. Phys.* **1998**, *109*, 10180.
- (36) (a) Dreuw, A.; Weisman, J. L.; Head-Gordon, M. *J. Chem. Phys.* **2003**, *119*, 2943. (b) Bernasconi, L.; Sprik, M.; Hutter, J. *J. Chem. Phys.* **2003**, *119*, 12417.
- (37) Yanai, T.; Tew, D. P.; Handy, N. C. *Chem. Phys. Lett.* **2004**, *393*, 51.
- (38) Becke, A. D. *Phys. Rev. A* **1988**, *38*, 3098.
- (39) Barker, J. W.; Noe, L. J. *J. Chem. Phys.* **1972**, *57*, 3035.
- (40) Fonseca, T. L.; Coutinho, K.; Canuto, S. *J. Chem. Phys.* **2008**, *129*, 034502.
- (41) (a) Kalinichev, A. G.; Bass, J. D. *J. Phys. Chem.* **1997**, *101*, 9720. (b) Malaspina, T.; Coutinho, K.; Canuto, S. *J. Chem. Phys.* **2002**, *117*, 1692. (c) Jorgensen, W. L.; Chandrasekhar, J.; Madura, J. D.; Impey, R. W.; Klein, M. L. *J. Chem. Phys.* **1983**, *79*, 926. (d) Rahman, A.; Stillinger, F. H. *J. Chem. Phys.* **1971**, *55*, 3336. (e) Mezei, M.; Beveridge, D. L. *J. Chem. Phys.* **1981**, *74*, 622. (f) Stillinger, F. H.; Rahman, A. *J. Chem. Phys.* **1972**, *57*, 1281. (g) Rapaport, D. C. *Mol. Phys.* **1983**, *50*, 1151.
- (42) DALTON, a molecular electronic structure program, Release 2.0. See <http://www.kjemi.uio.no/software/dalton/dalton.html>.
- (43) Tu, Y.; Laaksonen, A. *J. Chem. Phys.* **2000**, *113*, 11264.

JP809694W